January 2003 • NREL/SR-520-33278

Subcontractor Report

Plasma-Assisted Coevaporation of S and Se for Wide Band Gap Chalcopyrite Photovoltaics

Phase I Annual Report
December 2001–December 2002

I. Repins
ITN Energy Systems, Inc.
Littleton, Colorado

C. Wolden
Colorado School of Mines
Golden, Colorado

National Renewable Energy Laboratory

1617 Cole Boulevard
Golden, Colorado 80401-3393

NREL is a U.S. Department of Energy Laboratory
Operated by Midwest Research Institute • Battelle • Bechtel

Contract No. DE-AC36-99-GO10337

January 2003 • NREL/SR-520-33278

Plasma-Assisted Coevaporation of S and Se for Wide Band Gap Chalcopyrite Photovoltaics

Phase I Annual Report
December 2001–December 2002

I. Repins
ITN Energy Systems, Inc.
Littleton, Colorado

C. Wolden
Colorado School of Mines
Golden, Colorado

NREL Technical Monitor: H.S. Ullal

Prepared under Subcontract No. NDJ-2-30630-11

National Renewable Energy Laboratory

1617 Cole Boulevard
Golden, Colorado 80401-3393

NREL is a U.S. Department of Energy Laboratory
Operated by Midwest Research Institute • Battelle • Bechtel

Contract No. DE-AC36-99-GO10337

NOTICE

Available electronically at http://www.osti.gov/bridge

Available for a processing fee to U.S. Department of Energy
and its contractors, in paper, from:

U.S. Department of Energy
Office of Scientific and Technical Information
P.O. Box 62
Oak Ridge, TN 37831-0062
phone: 865.576.8401
fax: 865.576.5728
email: reports@adonis.osti.gov

Available for sale to the public, in paper, from:

U.S. Department of Commerce
National Technical Information Service
5285 Port Royal Road
Springfield, VA 22161
phone: 800.553.6847
fax: 703.605.6900
email: orders@ntis.fedworld.gov
online ordering: http://www.ntis.gov/ordering.htm

Printed on paper containing at least 50% wastepaper, including 20% postconsumer waste

TABLE OF CONTENTS

LIST OF FIGURES

LIST OF TABLES

1. Introduction, Goals, and Approach

In terms of small-area device efficiency and module stability $CuIn_xGa_{1-x}Se_2$ (CIGS) devices provide a benchmark for all thin film photovoltaics. Nonetheless, there is significant opportunity for improvement in manufacture of CIGS devices. First, high-quality CIGS deposition requires high substrate temperatures (>500°C), limiting the selection of substrate materials and increasing deposition cycle times due to heat-up and cool-down periods. Furthermore, current co-evaporation technology requires overpressure of chalcogens (Se_2 or S_2) during deposition, resulting in low material utilization and high equipment maintenance costs. Perhaps most important, the fundamental electrical properties of CIGS alloys limit the useful available energy bandgap to less than 1.3 eV.

In this work, ITN Energy Systems (ITN) and lower-tier subcontractor Colorado School of Mines (CSM) explore the replacement of the molecular chalcogen precursors during deposition (e.g. Se_2 or H_2Se) with more reactive chalcogen monomers or radicals (e.g. Se). Molecular species will be converted to atomic species in a low-pressure inductively-coupled plasma (ICP). The non-equilibrium environment created by the plasma will allow control over the S/Se ratio in these films. Tasks of the proposed program center on development and validation of monatomic chalcogen chemistry, tuning of low-pressure monomer chalcogen sources, and evaluation of plasma-assisted co-evaporation (PACE) for CIGS co-evaporation. Likely advantages of deposition by plasma-enhanced co-evaporation include:

- Provides potential for lower deposition temperature and/or for better film quality at higher deposition temperature.
- Provide potential for decreased deposition times.
- Provides high material utilization efficiency (~90%) that results in less deposition on other parts of the reactor leading to lower clean up and maintenance costs, as well as longer equipment lifetime. High material utilization efficiency also reduces the total operating pressure, which is beneficial for the design and control of metal co-evaporation. Advantages include minimal metal-vapor beam spread and lower source operating temperatures.
- Enables deposition of wide bandgap copper indium gallium sulfur-selenide (CIGSS) films with controlled stoichiometry.

University researchers at CSM are developing and testing the fundamental chemistry and engineering principles. Industrial researchers at ITN are adapting PACE technology to CIGSS co-evaporation and validating PACE process for fabrication of thin film PV. In_2Se_3 films, which are used as precursor layers in high-efficiency CIGS depositions, are being used as the first test case for the examining the advantages of PACE listed above. Eventually, this examination will be extended to the complete high-efficiency three-stage co-evaporation process.

2. Source Development

In the first year, the development of inductively couple plasma (ICP) sources has advanced mainly in the areas of hardware improvements, source operation, and source characterization, and film fabrication. Highlights of this year's work includes

- Successful operation of the ICP sources over wide ranges of pressures and power,
- Use of elemental Se and S as source feedstocks,
- Demonstration of the efficacy ICP sources in cracking N_2 and O_2 dimers,
- Modification of sulfur ICP source with consistent run-to-run deposition rate,
- Correlation of signals from mass spectrometry and optical emission spectroscopy for plasma characterization and rate monitoring, and
- Fabrication of first PACE $In_2(Se,S)_3$ films.

ICP Source Operation

ICP sources were operated in three different configurations and a over a wide range of operation conditions. The three configurations used for ICP source operation are shown in Figure 1. Figure 1a shows an ICP source operating in the CSM diagnostic chamber. The ICP source is the glowing quartz tube surrounded by a radio-frequency (RF) coil. Chalcogen vapors and Ar are fed into the tube outside the chamber. The RF plasma converts the stable vapors into highly active monomers and ions. The reactive species effuse from a small orifice at the end of the ICP device into the collision less high vacuum environment (10-5 Torr). The diagnostic chamber is used to examine the source characteristics for low chalcogen flows. The diagnostic chamber is fitted with advanced instrumentation such as an optical emission spectrometer (OES), a quadrupole mass spectrometer (QMS), and various gauging.

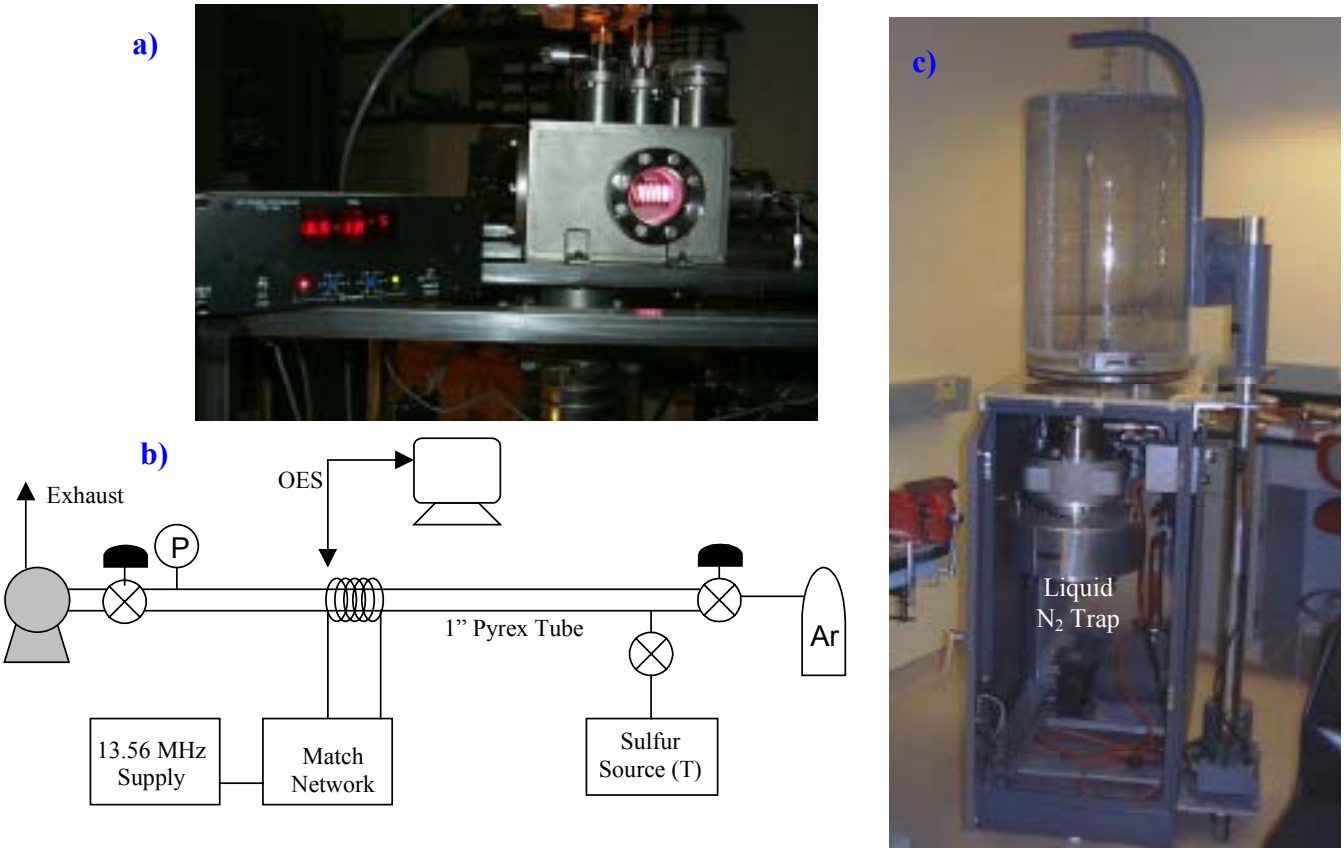

Figure 1: ICP source in a) diagnostic chamber, b) benchtop configuration, and c) PACE chamber.

Figure 1b shows a schematic of an ICP source operating in benchtop mode. This mode is useful for tests requiring significant chalcogen flux that would contaminate the advanced instrumentation in the diagnostic chamber. The plasma is contained in a 1" diameter pyrex tube. Argon is supplied through a needle valve, while an on/off valve isolates the chalcogen effusion source. A butterfly valve on the exhaust line is used to control the pressure. The effusion source is maintained at the desired temperature through PID control. This benchtop unit is operated at the similar conditions as will be used for CIGS film depositions. The only difference is that this system is exhausted directly to a pump, instead of effusing into a high vacuum environment. The benchtop plasma source allows extensive quantification of sulfur/selenium flux and optimization ICP operation as a function of pressure, power, and composition without contamination of other equipment.

The first simultaneous exposure of a substrate to the plasma-activated chalcogens, heat, and In was performed in the PACE chamber. The PACE chamber is shown in Figure 1c. This chamber is the next step in the transition of ICP sources to full CIGSS coevaporation. It allows the study of plasma-activated In_2Se_3 film formation and source uniformity without the stringent requirements on temperature and multi-source flux rate monitoring imposed by CIGSS co-evaporation. The PACE chamber includes a glass bell jar with implosion shield and hoist, a cabinet for housing pumps and instrumentation, a liquid trap, diffusion pump, and pneumatic gate valve. The baseplate was modified to accommodate the ICP sources and In evaporation.

A major improvement in ICP source operation was made with the elimination of RF leakage. The leakage had adverse implications for plasma tuning and the operation of other components. A prototype Faraday cage was designed, fabricated out of copper mesh, and implemented. The cage proved successful in eliminating RF noise to an undetectable level, an allowed tuning with near-zero reflected power. A permanent faraday cage was then constructed. In addition, improved RF connectors were obtained for both sides of the RF vacuum feedthrough. These improvements resulted in elimination of RF noise and reproducible ICP operation.

ICP Source Diagnostics

An important aspect of the ICP source operation is the ability to monitor deposition rate, chalcogen dissociation, and plasma characteristics such as plasma density and electron temperature. To achieve these functions, the interpretation of optical emission spectroscopy (OES) signals from the ICP sources is being developed simultaneously with the sources.

The use of OES on the ICP sources was first tested on the diagnostic chamber using O_2 and N_2 gases. Figure 2 shows OES spectra from the ICP source on the diagnostic chamber for different gas flows. Figure 2a shows the spectrum with O_2 flow only, and the source operated at 60W. Figure 2b shows the spectrum with N_2 flow only, and the source operated at 40W and 60W. In the spectra of Figure 2c, both gases are flowing through the source, and the characteristic peaks of each gas are evident.

The O_2 and N_2 OES spectra were then correlated with mass spectrometer data. The mass spectrometer (MS) was attached to the chamber and dual MS/ OES experiments are under way. MS signals are being cross-referenced with OES signals so that OES can be used as a real time sensor in future work. Efforts have been directed at quantifying the mass spectrometry. These have included the use of laser to align the MS and the ICP unit. A beam stop was purchased, modified and installed to distinguish ICP from background signal. The mass spectrometry data demonstrate the efficacy of the ICP sources in cracking gas species such as N_2 and O_2. Figure 3 and Figure 4 show MS data demonstrating the dissociation of oxygen and nitrogen dimers. When the plasma is ignited, the parent peaks - 32 and 28 respectively - decrease while the atomic peaks (16 and 14) increase. Table 2 shows a quantitative summary of the signal changes of the previous two figures. The relatively long transients associated with the data in Figure 3 and Figure 4 is attributed to heating of the ICP devices. This has been corroborated by simultaneous optical emission spectroscopy (OES) measurements.

Numerous data have been obtained on plasma dissociation efficiency. Work is underway to convert the raw data into quantitative measures of dissociation fraction. This involves calibrating the mass spectra peaks for differences in ionization efficiencies and cross sections. Further improvements in signal to noise ratio are also required before one can reliably report dissociation fractions. The MS signals shown in Figure 3 and Figure 4 arise from two sources: (1) the species emanating from the ICP device and (2)

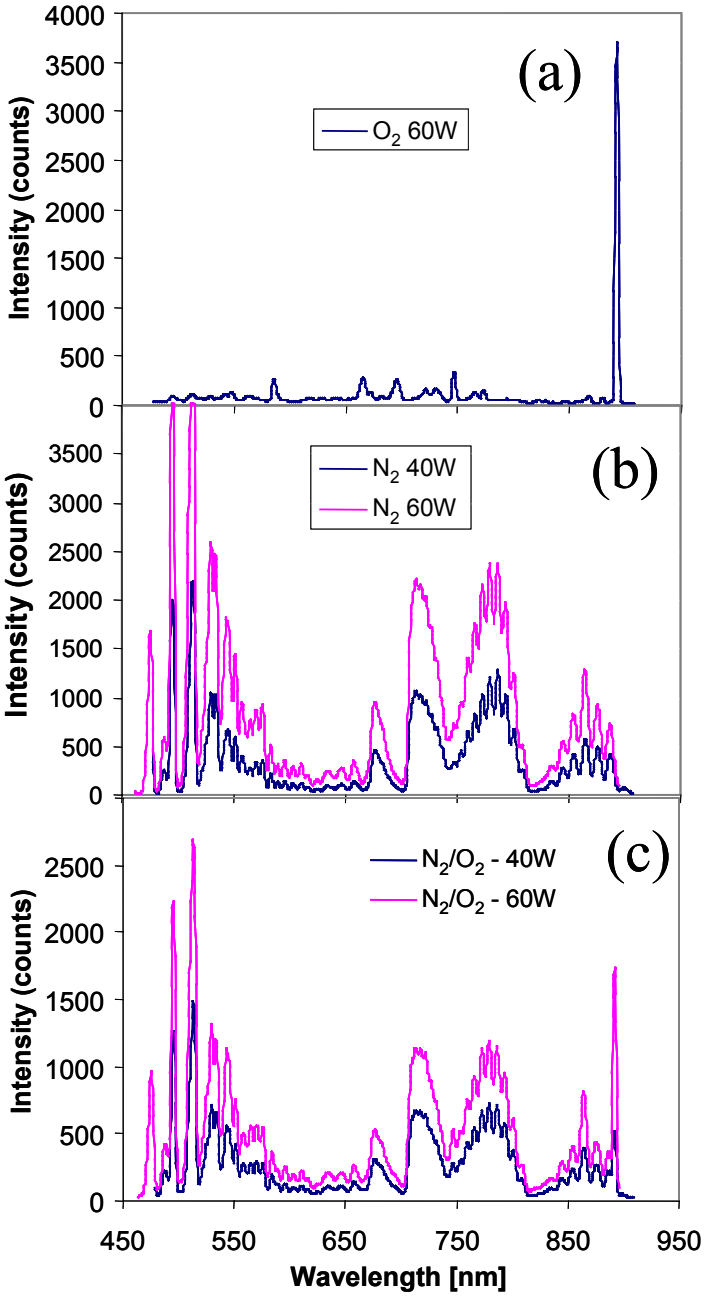

Figure 2 : OES spectra from ICP sources with flow of a) O_2, b) N_2, and c) both O_2 and N_2 gases.

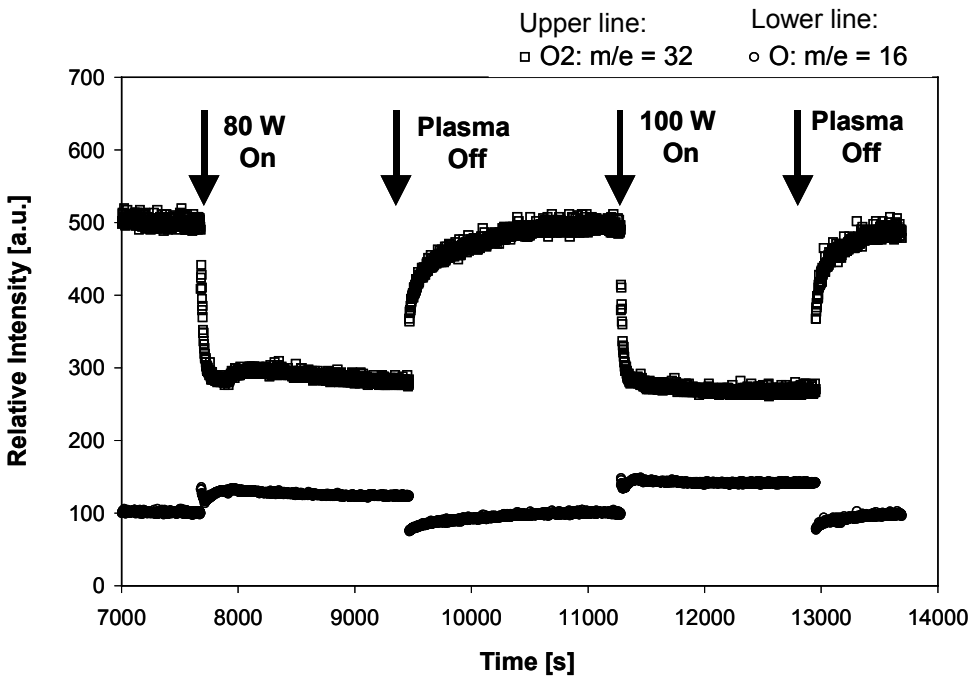

Figure 3: MS signals for an O_2 Plasma.

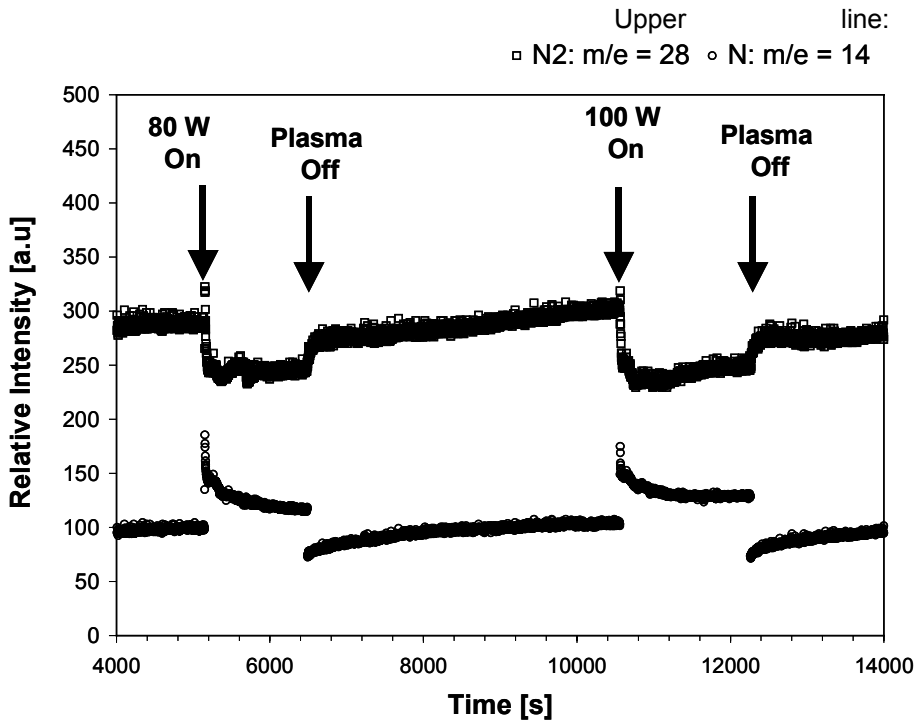

Figure 4: MS signals for a N_2 Plasma.

Signal	Change for a 80 W plasma	% Change for a 100 W plasma
O_2: m/e = 32	-42%	-46%
O: m/e = 16	+25%	+42%
N_2: m/e = 28	-16.5%	-20%
N: m/e = 14	+19%	+29%

Table 1: Summary of change in mass spectrometer signals for O_2 and N_2 plasmas.

background signal from gas species in the chamber. The individual contributions must be quantified before the data can be converted into quantitative measurements of percent dissociation. To do so, the following changes are being made:

- Making a series of ICP tubes with different orifice sizes. This will allow the same plasma to be created with different background pressure.
- Creating a second inlet into the chamber to leak controlled amount of background gas. Another manner of independently controlling the background signal.

These two techniques will allow us to turn the data into quantitative dissociation fractions.

ICP sources were operated in the benchtop configuration to examine delivery of S and Se. Figure 5 shows photographs of the source in operation with both an Ar plasma and an Ar/S plasma. A fiber optic based optical emission spectroscopy (OES) system was then used to characterize the plasmas. Representative OES spectra are shown in Figure 3. The S-containing plasma clearly shows the bands from 290-540 nm associated with the $B^3\Sigma^-$ transitions of electronically excited sulfur. The pyrex tube absorbs signal for wavelengths less than 350 nm. Stable sulfur/argon plasmas were obtained over a range of powers (30 – 100 W) with minimal reflected power (< 3 W), and the plasmas were stable over a large pressure range (20 – 200 mTorr). For most conditions the Pyrex wall remained clear (no S condenstion) throughout the majority of experiments. The exception was extremely high sulfur effusion temperatures.

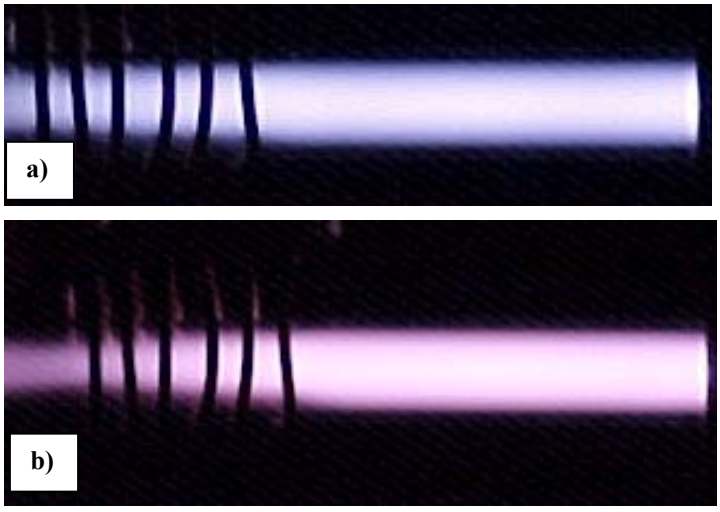

Figure 5: ICP source in operation with both a) Ar plasma, and b) Ar/S plasma.

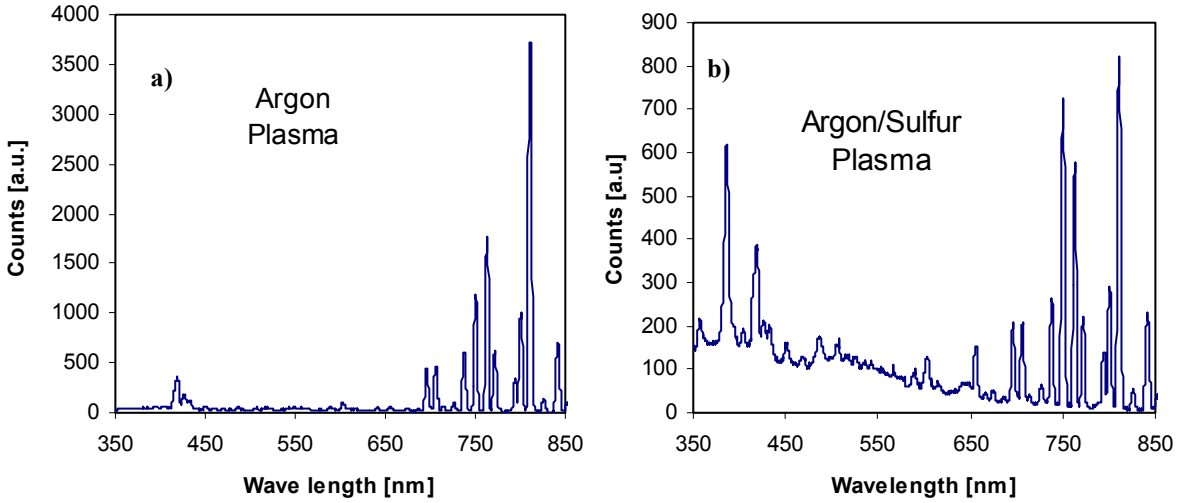

Figure 6: OES spectra of a) an Ar plasma and b) and Ar/S plasma.

Similar data were taken for the examination of Se delivery from the ICP source. A new source similar to the S source was fabricated for Se vaporization and the first Ar/Se plasma spectra was obtained. Figure 7 shows a representative spectrum. The main peaks of interest are in the region around 325-355 nm and a distinct peak at 376 nm. It is important to note that these peaks are out of the range of the S spectra, whose main peaks are located $400 < \lambda < 600$ nm. Thus, if both S and Se were activated in the same ICP source, the contributions of each chalcogen to the OES spectra could be deconvolved.

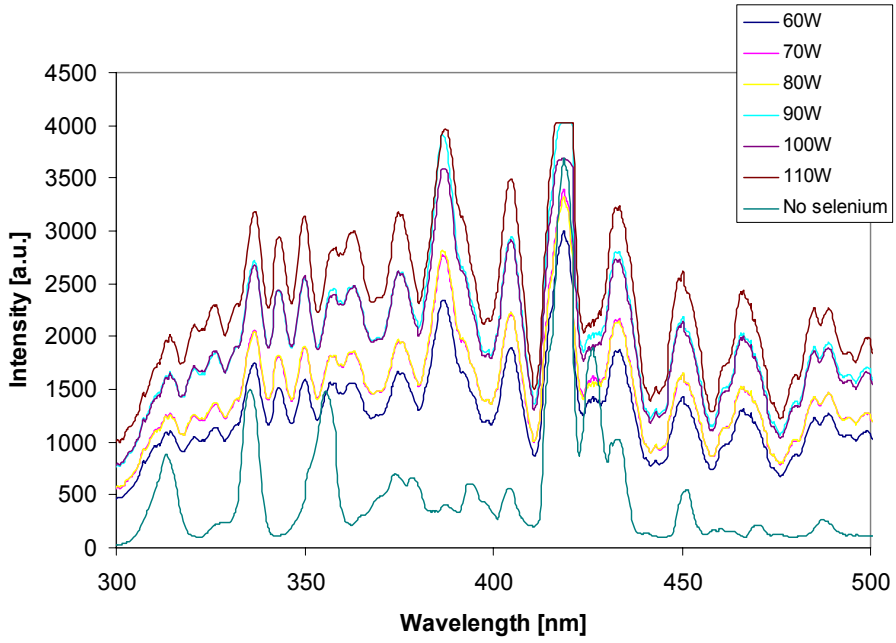

Figure 7: Se spectra versus power.

Work is currently underway to quantify S and Se flux as a function of temperature, effusion source design, and time - in a repeatable and continuous manner. The challenges to such quantification include both delivery of the source feedstock in a controllable manner, and accurate quantification of that flux.

For S, delivery of the source feedstock in a controlled manner is non-trivial. The S morphology changes dramatically upon condensation, impacting the surface area available for vaporization. As such, the energetics required to obtain a consistent vapor supply change from run to run. The process space and thermal evaporation source configurations that mitigate these issues are being explored. A new sulfur source was fabricated with a higher surface area/volume ratio for more rapid and reproducible temperature control. With this new configuration, reproducible and stable delivery of S vapor was achieved, as monitored by optical emission spectroscopy. Figure 8 shows the S spectra as a function of power. All signals increase monotonically with applied power.

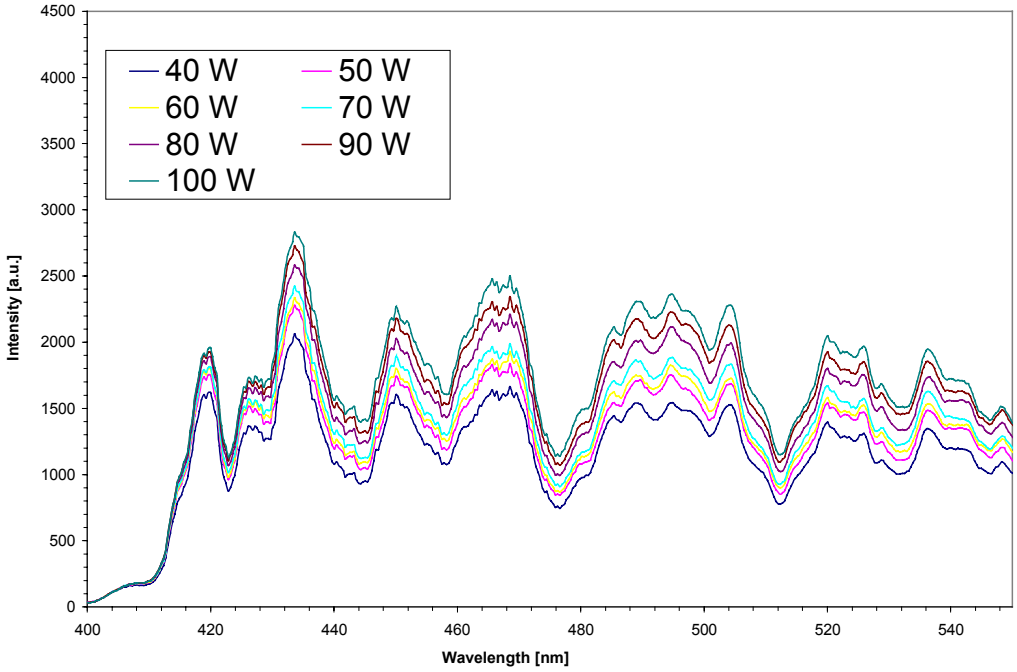

Figure 8: Sulfur emission spectra as a function of plasma power

Quantification of the S flux also requires some careful consideration. The S source temperature measurement is indirect. It is achieved through a thermocouple mounted outside the S source. As such, the absolute temperature of the sulfur source can vary from run to run. Similarly the absolute OES signal can vary with fiber optic placement and integration time. Actinometry is therefore under development, relying on ratio of S emission to Ar emission as the control metric for S and Se flux.

Figure 9 shows plots of actinometers versus control temperature. The S lines are at 450 and 468.5 nm, while the Ar actinometer line is 737 nm. Additional work needs to be done to establish exactly which S lines and which Ar lines are best for this application.

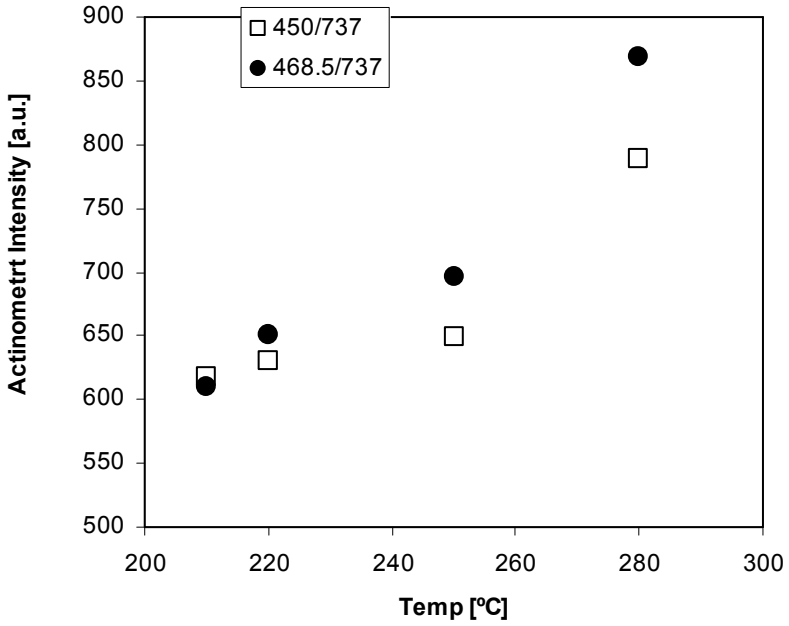

Figure 9: Actinometers vs. control temperature for S source

PACE films

In order to make the first PACE In_2Se_3 films, the PACE chamber, as described earlier, was completely assembled with all the components required to demonstrate the PACE process. Such components include a baseplate, collar, quartz bell jar, diffusion pump, mechanical pump, substrate holder, radiative substrate heating assembly, three thermocouples for monitoring and active feedback control of substrate temperature, ICP source for the dissociation of S and Se vapors carried by Ar carrier gas, 300 watt RF power supply and matching network, evaporation boat for indium shot, and low voltage/high current transformer.

Preliminary PACE $In2(Se,S)_3$ samples were prepared, meeting the first year milestones. The samples were prepared on glass substrates though the simultaneous exposure to heat, plasma-activated sulfur and selenium, and indium. The sulfur and selenium vapor were sublimed from solid sources and carried into the reactor by argon.

A photograph of one sample is shown in Figure 10. The results are encouraging, considering that these were preliminary experiments with poor control of the various process variables. The morphology at the center of the sample is visually similar to In_2Se_3 films that were produced at ITN by thermal co-evaporation. In the upper corner and on the edges there are regions of no or little In, and these regions have a reddish-gold hue that implies unreacted condensed chalcogen. The XRD facility at CSM has recently been unavailable due to repairs and maintenance, so more detailed structural evaluation on these films has not yet been performed.

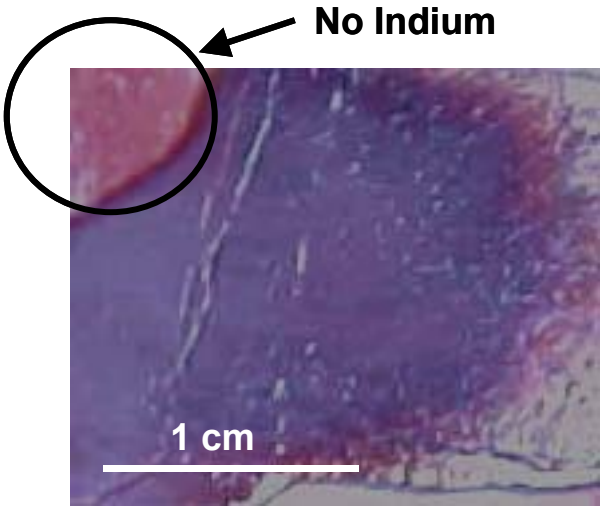

Figure 10: Photograph of preliminary In-Se-S sample produced by PACE. The red area in the upper left hand area was not exposed to indium and is simply condensed chalcogen vapors.

Several issues must be addressed in the fabrication of the PACE In_2Se_3 film. As stated above, the process conditions have not been well controlled or characterized in the initial experiments to date. Improving the control and reproducibility will be the focus of our efforts in the next months. Specific issues that will be addressed include the following:

- *Improve Vacuum Integrity*: Having rapidly assembled the PACE chamber, there were minor leaks remaining that must be eliminated. The current base pressure is ~ 10^{-6} torr. After tracking down the minor leaks this will be reduced by an order of magnitude.
- *Calibrate indium flux*: At the start of Phase II we will purchase a film thickness monitor to calibrate and control the indium evaporation rate.
- *Improved Chalcogen Delivery*: The current method of chalcogen delivery is suboptimal. Currently we pass cold argon through a heated effusion source. There are two major deficiencies with this approach. First, since the gas temperature is always less than the source temperature ($T_g < T_s$), it is inherently susceptible to nucleation and condensation. Second, due to the thermal mass of the effusion source and the heating arrangements the time constants are too slow. Thus it very easy to overshoot desired effusion set point. Due to the exponential dependence of vapor pressure this results in excessive chalcogen flux and condensation in the ICP source. As discussed in previous reports optical emission is a very good real-time sensor for this phenomenon, however real-time control is not possible due to the slow dynamics of the limited effusion source.

  The proposed solution is to reverse the process: have a cold chalcogen source and heat the carrier gas. This has two profound advantages. First, the gas temperature is always greater than the source ($T_g > T_s$), eliminating the possibility of gas-phase nucleation and condensation. Second, the time constants are much shorter. Gas heating will be achieved using immersion heaters that work by transporting the gas across resistively heated wires. The rapid response of both the heating elements and the low thermal mass of the gas allows for rapid turn on, turn off, and enable real time control. The source tubes would be prepared by loading a known amount of chalcogen in a tube, purging it with argon, and sealing it. It would then be put into a furnace where it will be slowly heated and cooled, vaporizing the chalcogen and allowing it to recondense as a uniform film on the inside of the tube. This is analogous to the preparation of source plates used for CdTe deposition or $CdCl_2$ treatment in close space sublimation. Figure 11 contrasts the two approaches just described.

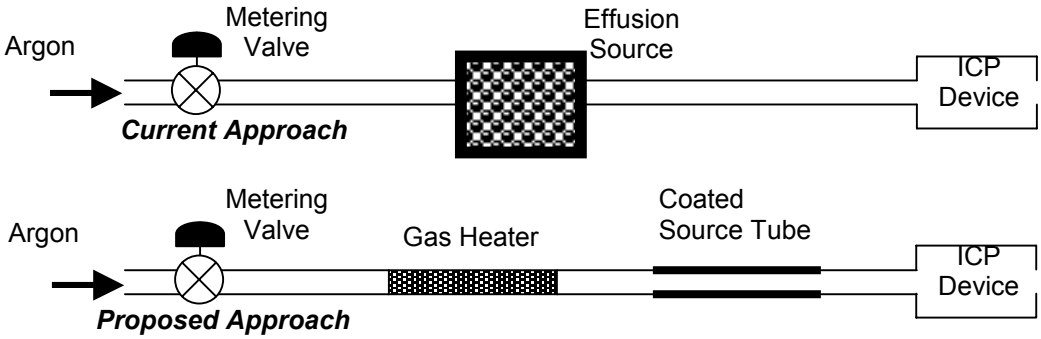

Figure 11: Schematic comparison of approaches for chalcogen delivery.

- *Calibrate Substrate Temperature*: The radiative heater assembly delivers rapid control of substrate temperature up to at least 600 ºC. The heaters are controlled by a thermocouple that is permanently mounted on the substrate holder next to the substrate. Thus there is some offset between the control temperature and the true substrate temperature, which must be calibrated. An assessment of the temperature uniformity is also necessary. The uniformity can be improved, if necessary, by adjusting the distance between the heater assembly and the substrate holder. The optimum distance will reflect a balance between uniformity and response time.
- *Integrate Control & Data Acquisition*: At present individual controllers handle the various aspects of the projects. In Phase II the use Labview is planned to integrate the controllers, enable data acquisition, and allow recipes to be programmed.

3. Baseline Process

A CIGS co-evaporation process in a bell jar was established. This standard process provides co-evaporated films to compare with the PACE films made at CSM, and will eventually serve as a testbed for integration of PACE into three-stage CIGS co-evaporation. This section documents the work that completes a first-year milestone: demonstrating CIGS co-evaporation baseline with chalcogen rate monitoring, and a 50% yield of devices with efficiency over 10%.

The bell jar design is based on that of the NREL CIGS evaporators, and was assembled at ITN. Evaporation of the elements is performed through resistive heating of small Cu, In, Ga, and Se boats, each with a capacity of several grams. Se rate is monitored by quartz crystal microbalance (QCM), and metals rates are monitored by electron impact emission spectrometry (EIES). The substrate is heated radiatively, and its temperature is monitored by thermocouple. Figure 12 shows two views of the bell jar. Figure 12a uses a cut-out view of the bell jar exterior to show the positioning of the EIES emission head relative to the deposition zone. Figure 12a utilizes a cut-out view to show the deposition zone - and the position of the EIES relative to it - with the bell jar down. The evaporation boats are located near the bottom of the cut-out. The substrate heaters and thermocouple are visible at the top of the cut-out. A copper-colored shutter is seen shielding the substrate in the top 1/3 of the cut-out. The location of the EIES emission head is level with the black photomultiplier tubes at the right of the photo. Figure 12b shows the EIES emission head affixed to the inside of the bell jar, as the bell jar descends from the open position into its deposition position on the base plate.

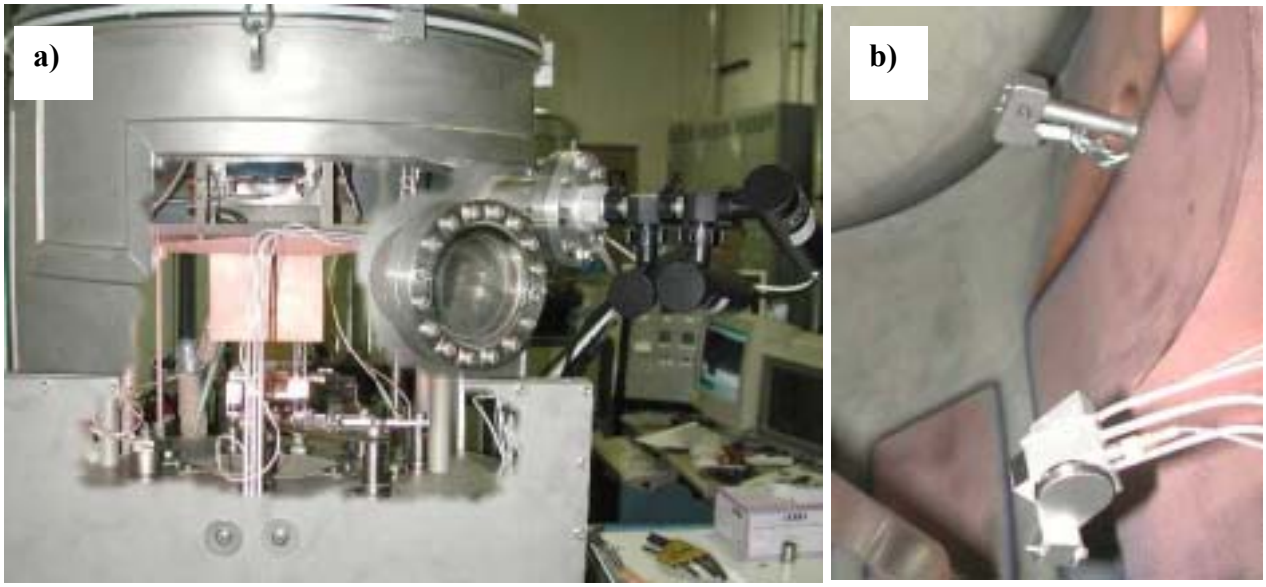

Figure 12: Photographs of co-evaporation baseline bell jar a) with cut-out showing deposition zone and positioning of components with lid down, and b) showing EIES head position relative to bell jar wall.

Several adjustments were made to the bell jar and its operating procedure with the first CIS runs. These include adjustments include installation of cooling along the tube from the EIES filament to the EIES signal window to prevent coating the window with Se, shielding the Se QCM and the EIES from radiation from the substrate heaters, tuning proportional-integral-derivative (PID) parameters on the sources, implementation of automatic recipes to improve reproducibility and reduce operator error, and implementation of a chamber bake-out to reduce noise in the Ga signal during the second and third stages. Temperature uniformity of the substrate was also examined, and determined to be satisfactory. Flux profiles and temperatures were programmed to follow the NREL three-stage process[1], as shown in Figure 13. Films show the expected change in emissivity[2] during the third stage, as composition changes from Cu-rich to Cu-poor. Substrate temperature is actively-controlled, so the emissivity change is evidenced by an increase in substrate heater power, and a slight dip in temperature as the power is adjusted. These data are shown in Figure 14.

[1] A.M. Gabor, J.R. Tuttle, D.S. Albin, M.A. Contreras, R. Noufi, "High Efficiency $CuIn_xGa_{1-x}Se_2$ Solar Cells Made from $(In_x, Ga_{1-x})_2Se_3$ Precursor Films," *Appl. Phys. Lett.*, **65** (2) 1994, pp. 198-200.

[2] J. Kessler, J. Scholdstrom, L. Stolt, "Rapid Cu(In,Ga)Se^2 Growth Using 'End Point Detection' ", *Proceedings of the 28th IEEE Photovoltaic Specialists Conference*, 2000, pp. 509-512.

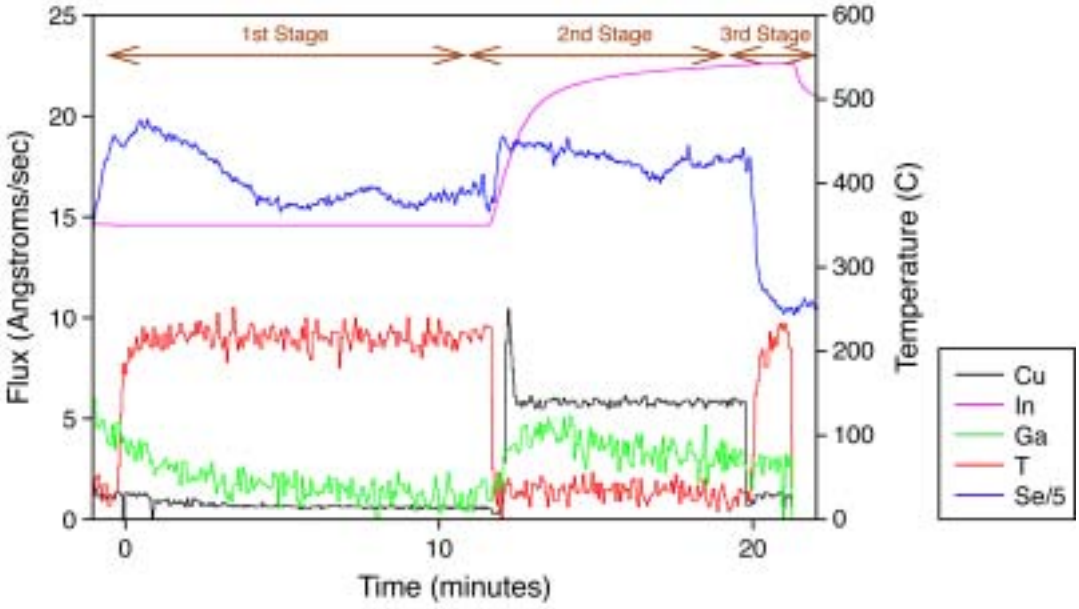

Figure 13 : Time, temperature, and deposition flux profiles for CIS deposition.

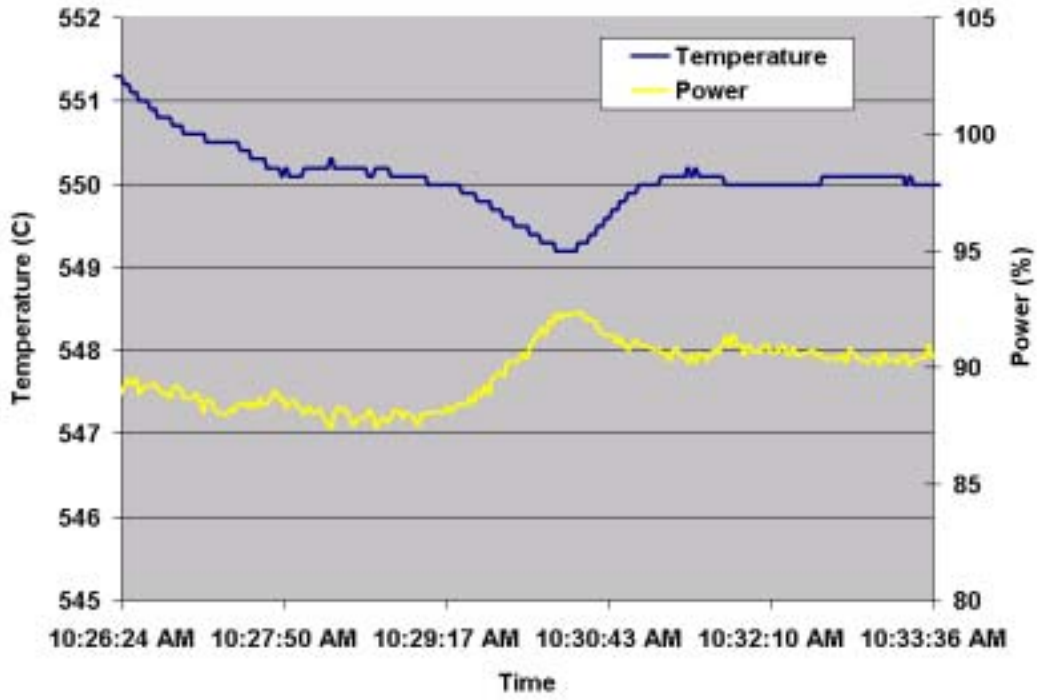

Figure 14 : Deposition temperature and power at Cu-rich/Cu-poor transition.

CIS depositions were shown to be repeatable in composition for constant deposition conditions. This repeatability is demonstrated by the data is shown in Figure 15. After each deposition, Cu and In content of the film was measured via x-ray fluorescence (XRF). For a reproducible deposition, the content of the Cu and In in the film should correspond the rate monitor (EIES) signal integrated over the

deposition. Figure 15 shows, for a series of recent depositions, the actual Cu content of the film divided by the integrated Cu rate monitor signal over the deposition. The same information is shown for In. For constant deposition temperatures, the ratio is constant, indicating a reproducible deposition.

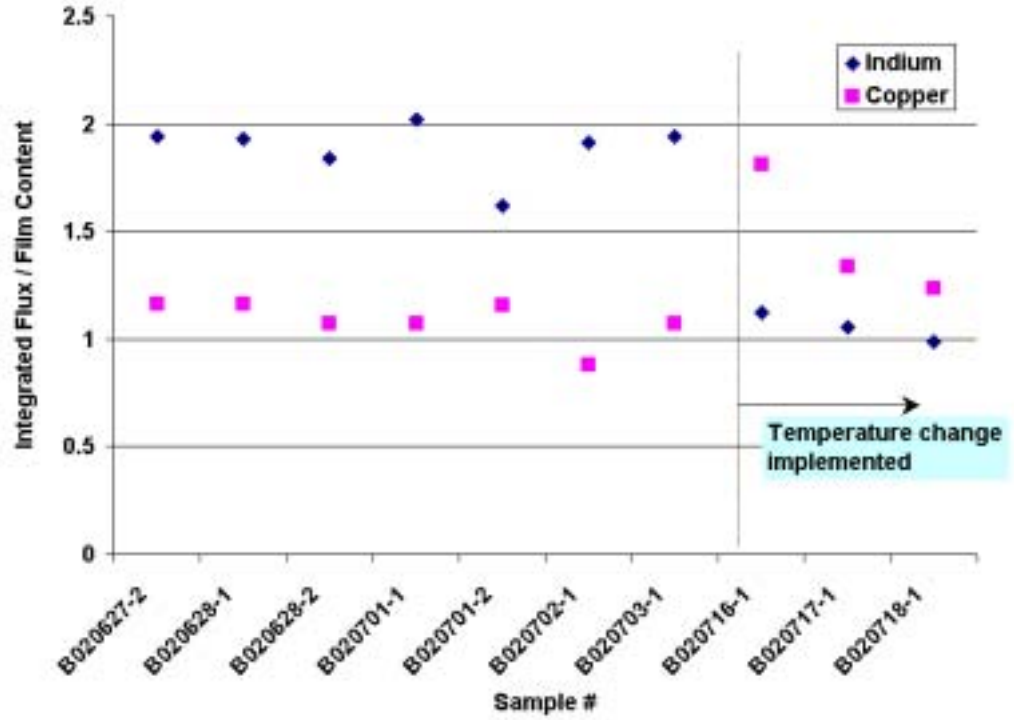

Figure 15: Predicted vs. measured film composition for multiple CIS films.

Device results on CIS films (without Ga) are fairly uniform over the 3" x 3" substrate, as well as being reproducible from run to run. Over the most recent seven CIS depositions, maximum CIS device efficiency on each substrate ranged from 7.3% to 8.8%. These devices are 1 cm^2, contain no Ga, and are not treated with an antireflective coating. Uniformity in device efficiency is typically around ±1% over the 50 devices produced on each 3" x 3" substrate. For example, on substrate B020822, average device efficiency was 7.9%, with a 6.8% lowest efficiency, and an 8.7% highest efficiency.

As expected, the incorporation of Ga into the devices increases device efficiency due to a better match of the absorber bandgap to both the solar spectrum and the indium tin oxide transmission. CIGS devices to date have been fabricated with a maximum efficiency of 10.9%.

Improvement in device uniformity over each substrate is needed for devices containing Ga. Figure 16 shows a device efficiency map over a 2"x2" area for CIGS depositions producing 10.9% and 10.4% highest efficiency devices. A large fraction of the devices on the substrate are below 8%. It was determined that – due to a ~10% compositional gradient over the 3" x 3" substrate – the high-efficiency side of the substrate goes Cu-rich during the second stage of the three-stage process, whereas the low efficiency side does not. On the low-efficiency side of the substrate, SEM shows much smaller grains, and quantum efficiency (QE) exhibits red loss consistent with low diffusion length. The existing deposition procedure will be modified to include more In in the third stage, so that the entire substrate goes Cu-rich. A robust calibration procedure is being established prior to this fine-tuning of the flux delivery.

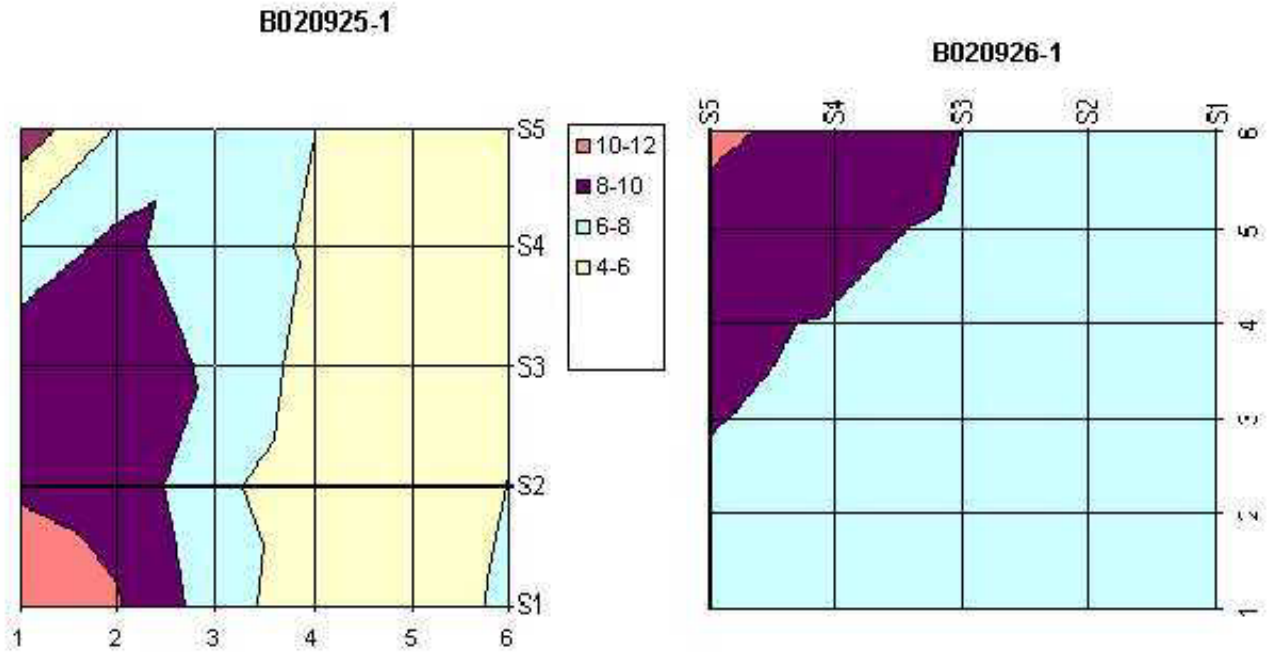

Figure 16: Device efficiency map over 2"x2" area for CIGS depositions producing 10.9% (B20925-1) and 10.4% highest efficiency devices.

4. Film Characterization

The previous section described establishing a three-stage bell jar process. The bell-jar process was used to fabricate In_2Se_3 films under both standard and non-standard conditions. Since goals of the PACE process are decreased deposition temperatures, increased Se utilization, and decreased deposition time, the In_2Se_3 films were deposited as a function of In/Se flux ratio, deposition temperature, and deposition rate. The films were then characterized by several techniques in order to determine a good metric of film quality. The films were characterized by x-ray fluorescence (XRF), x-ray diffraction (XRD), and scanning electron micrograph. Each of these characterization techniques demonstrated characteristics of the film related to varying deposition temperature and Se flux. Films made with low Se flux exhibited lower Se content in XRF measurements, Se-deficient phases in XRD measurements, and reduced grain size in SEM measurements. Films made at lower temperatures exhibited reduced grain sizes in SEM, and wider In_2Se_3 peaks in XRD. Successful PACE In_2Se_3 films made in the next phase will show the same grain sizes, compositions, and XRD peak widths when made at a lower temperatures and Se fluxes.

Under standard conditions (i.e. those typically used in the first stage of the three-stage recipe), all peaks in the XRD pattern can be assigned to In_2Se_3. An example of a standard In_2Se_3 XRD pattern is shown in Figure 17. With changes in deposition temperature, and decreasing Se/In flux, peaks associated with Se-deficient phases, including InSe, In_4Se_3, and In, become apparent.

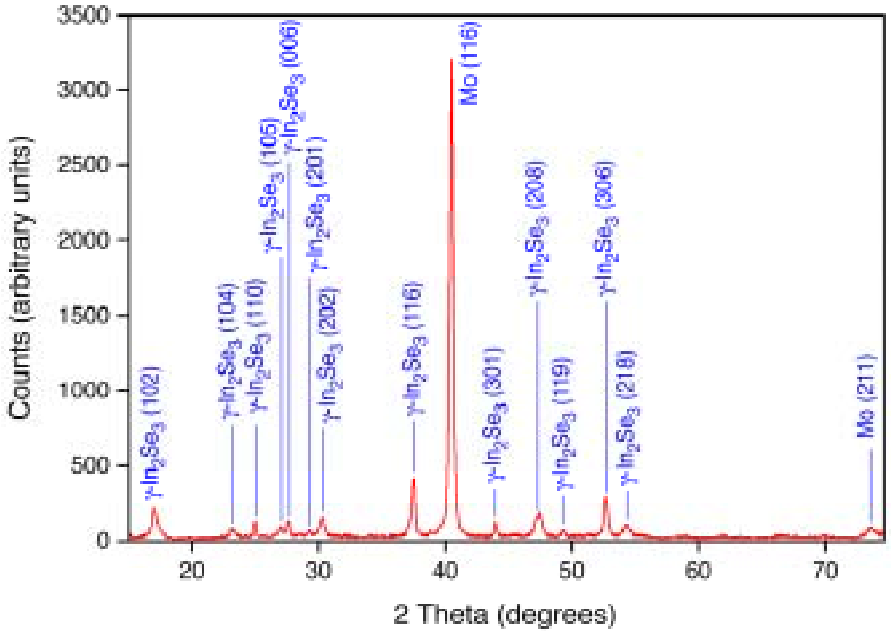

Figure 17: XRD pattern from standard co-evaporated In_2Se_3 film, with peak assignments.

Further analysis of the XRD data shows a correlation between some γ-In_2Se_3 widths and In_2Se_3 deposition temperature, as would be expected of an indicator of the film crystallinity. This relationship is shown in Figure 18 for the γ-In_2Se_3 (202) reflection at $2\theta=30.4^o$. The four films in the series in which Se-poor phases were evident did not demonstrate this reflection, and are therefore not included on the graph.

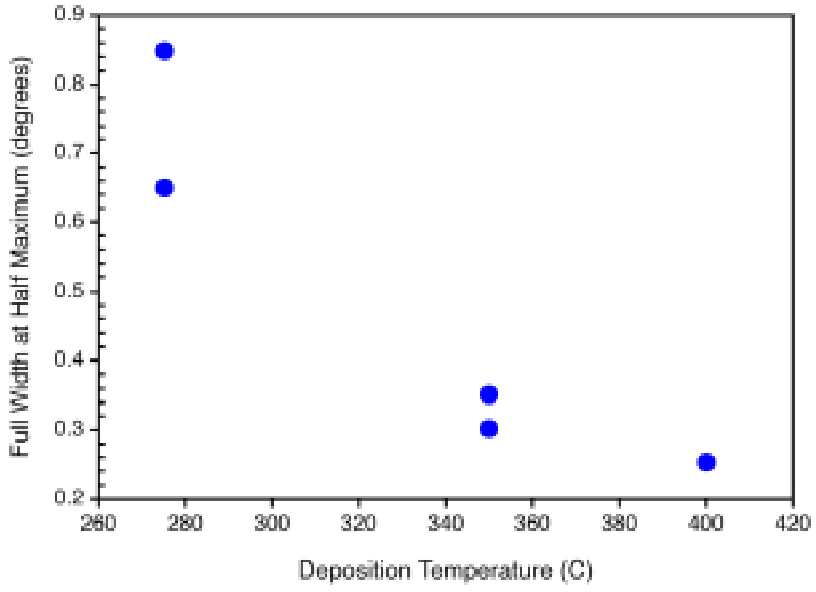

Figure 18: γ-In_2Se_3 (202) peak width versus film deposition temperature.

SEM characterization was also performed on the series of In_2Se_3 films. Decreased feature size was found to be associated with lower temperature and lower Se flux. An example of this correlation is shown in the SEM photos Figure 19. Figure 19a shows a 20,000x micrograph of a standard In_2Se_3 film (350 ^oC substrate temperature). In Figure 19b, a film made at higher temperature (400 ^oC) is shown, and a slightly larger feature size is evident. Figure 19c shows a film made at lower temperature (275 ^oC), with smaller grains. When both temperature and Se flux are decreased, grain size deteriorates further still, as seen in Figure 19d.

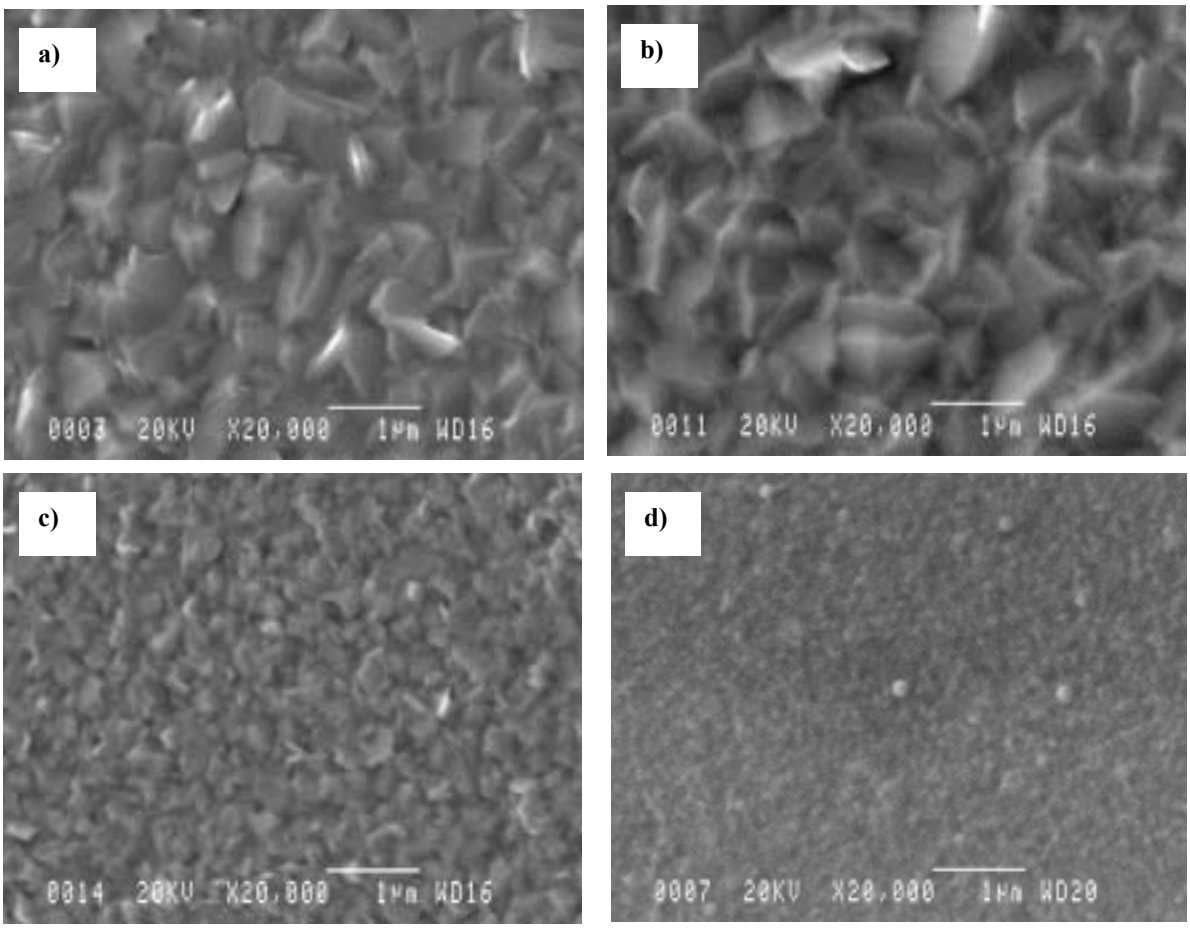

Figure 19: SEM photos SEM photos of In_2Se_3 films under the following conditions: a) standard, b) elevated temperature, c) decreased temperature, and d) decreased temperature and Se flux.

Figure 20 shows the grain size of all the In_2Se_3 films in the series as a function of substrate temperature and Se/In flux to the substrate. Grain size increases both with substrate temperature and with Se/In flux.

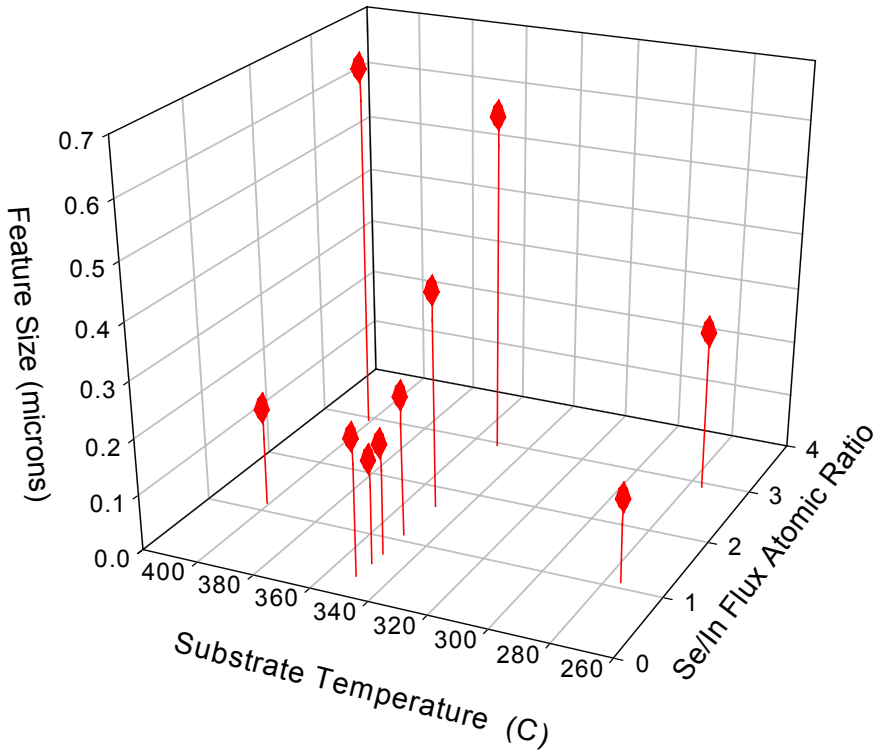

Figure 20: Grain size of In_2Se_3 films as a function of substrate temperature and Se/In flux to substrate.

Table 2 summarizes the deposition conditions and main characterization features of the In_2Se_3 films studied during Phase I. In Table 2, the Se/In atomic ratio in the film (sixth column) was measured by XRF. Standard deviation for the XRF measurements is shown, based on counting statistics for the two-minute measurement period. In some samples, XRD detected Se-deficient phases (seventh column). Note that Se-deficient phases were detected in all in samples with a Se/In composition less than 1.5 minus the measurement uncertainty, and only in those samples. In samples without Se-deficient phases, narrow XRD peak widths (ninth column) and large SEM grain sizes (tenth column) correlate with adequate deposition temperature and Se flux. No dependence of film properties on In deposition rate (for a fixed Se/In flux ratio) was apparent over the limited range examined. It is likely that for evaluating PACE In_2Se_3 film, SEM feature size will be a key indicator. A successful PACE films should exhibit the same grain size as traditionally co-evaporated In_2Se_3 films made at higher Se fluxes and higher temperatures.

Row	Sample ID	Description	Temper-ature (C)	In Flux (Å/sec)	Se/In Atomic Flux Ratio	Se/In Atomic Ratio in Film	Se-Deficient Phases Detected	202 Peak Width (degrees)	Grain Size (μm)
1	B020813-1	Standard	350	13.2	2.9	1.55 ± 2.0%	No	0.35	0.61
2	B020814-1	Increased T	400	13.2	2.9	1.55 ± 2.2%	No	0.25	0.66
3	B020814-2	Decreased T	275	13.2	2.9	1.55 ± 2.1%	No	0.85	0.29
4	B020722-2	Low Se	350	6.7	1.1	1.49 ± 2.5%	No	0.35	0.25
5	B020722-1	Low Se, increased T	400	6.7	1.1	1.20 ± 2.2%	Yes	Not present	0.18
6	B020723-1	Low Se, decreased T	275	6.7	1.1	1.46 ± 2.3%	Yes	0.65	0.15
7	B020729-2	Moderately low Se	350	6.7	1.7	1.51 ± 2.3%	No	0.30	0.39
8	B020729-1	Very low Se, high In rate	350	15	0.75	1.10 ± 1.6%	Yes	Not present	$\leq$ 0.2
9	B020725-1	Further reduced Se	350	6.7	0.56	0.97 ± 2.3%	Yes	Not present	< 0.2
10	B020726-1	Further reduced Se	350	6.7	0.29	0.54 ± 2.3%	Yes	Not present	0.25

Table 2: Summary of deposition conditions and main characterization features of co-evaporated In_2Se_3 films.

5. Team Activities

ITN CIS team activities have included facilitation of absorber sub-team activities, discussion of and comparative analysis of results, and attendance at team meetings.

6. Conclusions

During Phase I,

- ICP sources were successfully operated over wide ranges of pressures and power.
- Elemental Se and S, were all used as feedstocks for the ICP sources.
- The efficacy ICP sources in cracking N_2 and O_2 dimers was proven.
- Design of the S ICP source was modified to yield consistent run-to-run deposition rate.
- No coating of ICP sources was evident except at the highest S deposition rate.
- Signals from mass spectrometry and optical emission spectroscopy were correlated for plasma characterization and rate monitoring.
- The first plasma-activated $In_2(Se,S)_3$ films were fabricated, as first-year research target.

- The effect of reduced temperature and Se flux on In_2Se_3 films was evident in SEM and XRD characterization, in the form of reduced grain size, increased reflection width, and the appearance of Se-deficient phases.
- A baseline bell-jar process was established to provide standard films to compare with PACE films, and to serve as a testbed for integration of PACE into CIGSS. Device-quality CIGS films were fabricated with high yield, a first-year research target.
- Uniformity on baseline CIS is good, while uniformity of baseline CIGS needs improvement.

7. Future Directions

Future work under this contract includes both new tasks to further the development of PACE, and tasks suggested as follow-ups to this year's work. New tasks for Phase II include

- **Specifying effectiveness of PACE for increasing materials utilization and decreasing reaction temperature during In_2Se_3 fabrication.** This task involves a comparison of PACE films at reduced Se flux and deposition temperature with standard In_2Se_3. Measurements of film quality based on SEM and XRD were developed during Phase I.
- **Report comparison of chalcogen source geometry, control, reliability, and flux spatial uniformity necessary for CIGSS film deposition with current ICP source operating conditions.** Constraints on ICP characteristics for successful integration into the baseline process shall be specified. The required characteristics will be compared with those measured on the current source design.
- **Identify plan for incorporation of ICP sources into CIGS baseline chamber.** Materials and components necessary to incorporate ICP sources into baseline chamber shall be identified and designed.

A number of specific items must be performed as follow-ups to this year's results. Such items include, as discussed in the main text of the report,

- Improve vacuum integrity of the PACE chamber.
- Calibrate the In flux in the PACE chamber.
- Improve chalcogen delivery in the PACE chamber via use of a hot carrier gas.
- Calibrate PACE chamber substrate temperature and adjust for good uniformity.
- Integrate control and data acquisition on PACE chamber.
- Establish which S lines and which Ar lines are best for chalcogen actinometry, and demonstrate that it is an acceptable method of rate monitoring.
- Convert MS and OES data into quantitative measures of dissociation fraction.
- Improve EIES calibration procedure
- Improve uniformity in CIGS devices in baseline process by making sure the entire substrate undergoes a Cu-rich phase.

REPORT DOCUMENTATION PAGE

Form Approved
OMB NO. 0704-0188

1. AGENCY USE ONLY (Leave blank)	2. REPORT DATE	3. REPORT TYPE AND DATES COVERED
	January 2003	Phase I Annual Report December 2001 – December 2002

4. TITLE AND SUBTITLE
Plasma-Assisted Coevaporation of S and Se for Wide Band Gap Chalcopyrite Photovoltaics: Phase I Annual Report, December 2001 – December 2002

5. FUNDING NUMBERS
PVP35001
NDJ-2-30630-11

6. AUTHOR(S)
I. Repins[1] and C. Wolden[2]

7. PERFORMING ORGANIZATION NAME(S) AND ADDRESS(ES)
1. ITN Energy Systems, Inc.
8130 Shaffer Parkway
Littleton, Colorado 80127-4107
2. Colorado School of Mines
Golden, Colorado 80401

8. PERFORMING ORGANIZATION REPORT NUMBER

9. SPONSORING/MONITORING AGENCY NAME(S) AND ADDRESS(ES)
National Renewable Energy Laboratory
1617 Cole Blvd.
Golden, CO 80401-3393

10. SPONSORING/MONITORING AGENCY REPORT NUMBER
NREL/SR-520-33278

11. SUPPLEMENTARY NOTES
NREL Technical Monitor: H.S. Ullal

12a. DISTRIBUTION/AVAILABILITY STATEMENT
National Technical Information Service
U.S. Department of Commerce
5285 Port Royal Road
Springfield, VA 22161

12b. DISTRIBUTION CODE

13. ABSTRACT *(Maximum 200 words):* In this work, ITN Energy Systems (ITN) and lower-tier subcontractor Colorado School of Mines (CSM) explore the replacement of the molecular chalcogen precursors during deposition (e.g., Se_2 or H_2Se) with more reactive chalcogen monomers or radicals (e.g., Se). Molecular species will be converted to atomic species in a low-pressure inductively coupled plasma. The non-equilibrium environment created by the plasma will allow control over the S/Se ratio in these films. Tasks of the proposed program center on developing and validating monoatomic chalcogen chemistry, tuning of low-pressure monomer chalcogen sources, and evaluating plasma-assisted coevaporation (PACE) for CIGS coevaporation. Likely advantages of deposition by plasma-enhanced coevaporation include:

- Provides potential for lower deposition temperature and/or for better film quality at higher deposition temperature.
- Provide potential for decreased deposition times.
- Provides high material utilization efficiency (~90%) that results in less deposition on other parts of the reactor, leading to lower clean-up and maintenance costs, as well as longer equipment lifetime.
- High material utilization efficiency also reduces the total operating pressure, which is beneficial for the design and control of metal coevaporation. Advantages include minimal metal-vapor beam spread and lower source operating temperatures.
- Enables deposition of wide-bandgap copper indium gallium sulfur-selenide (CIGSS) films with controlled stoichiometry.

14. SUBJECT TERMS: PV; inductively couple plasma (ICP); radio-frequency; optical emission spectrometer (OES); quadrupole mass spectrometer (QMS); plasma-assisted coevaporation; proportional-integral-derivative; quantum efficiency; wide bandgap chalcopyrite

15. NUMBER OF PAGES

16. PRICE CODE

17. SECURITY CLASSIFICATION OF REPORT	18. SECURITY CLASSIFICATION OF THIS PAGE	19. SECURITY CLASSIFICATION OF ABSTRACT	20. LIMITATION OF ABSTRACT
Unclassified	Unclassified	Unclassified	UL